# Nuclear magnetic resonance shielding constants and chemical shifts in linear $^{199}$Hg compounds: A comparison of three relativistic computational methods

Vaida Arcisauskaite,[1,a)] Juan I. Melo,[2] Lars Hemmingsen,[1] and Stephan P. A. Sauer[3]

[1]*Department of Basic Sciences and Environment, Faculty of LIFE Sciences, University of Copenhagen, Thorvaldsensvej 40, DK-1871 Frederiksberg, Denmark*
[2]*Departamento de Física, Facultad de Ciencias Exactas y Naturales, Universidad de Buenos Aires, Ciudad Universitaria, Pab. 1, 1428 Buenos Aires, Argentina and CONICET*
[3]*Department of Chemistry, University of Copenhagen, Universitetsparken 5, DK-2100 Copenhagen Ø, Denmark*

We investigate the importance of relativistic effects on NMR shielding constants and chemical shifts of linear $HgL_2$ (L = Cl, Br, I, $CH_3$) compounds using three different relativistic methods: the fully relativistic four-component approach and the two-component approximations, linear response elimination of small component (LR-ESC) and zeroth-order regular approximation (ZORA). LR-ESC reproduces successfully the four-component results for the C shielding constant in $Hg(CH_3)_2$ within 6 ppm, but fails to reproduce the Hg shielding constants and chemical shifts. The latter is mainly due to an underestimation of the change in spin-orbit contribution. Even though ZORA underestimates the absolute Hg NMR shielding constants by $\sim$2100 ppm, the differences between Hg chemical shift values obtained using ZORA and the four-component approach without spin-density contribution to the exchange-correlation (XC) kernel are less than 60 ppm for all compounds using three different functionals, BP86, B3LYP, and PBE0. However, larger deviations (up to 366 ppm) occur for Hg chemical shifts in $HgBr_2$ and $HgI_2$ when ZORA results are compared with four-component calculations with non-collinear spin-density contribution to the XC kernel. For the ZORA calculations it is necessary to use large basis sets (QZ4P) and the TZ2P basis set may give errors of $\sim$500 ppm for the Hg chemical shifts, despite deceivingly good agreement with experimental data. A Gaussian nucleus model for the Coulomb potential reduces the Hg shielding constants by $\sim$100–500 ppm and the Hg chemical shifts by 1–143 ppm compared to the point nucleus model depending on the atomic number $Z$ of the coordinating atom and the level of theory. The effect on the shielding constants of the lighter nuclei (C, Cl, Br, I) is, however, negligible. © *2011 American Institute of Physics*. [doi:10.1063/1.3608153]

## I. INTRODUCTION

The coordination chemistry of Hg(II) is important in its own right, and, in particular, because mercury ions may substitute native metal ions in metalloproteins, probably giving rise to the well known toxic effects of this heavy metal ion. $^{199}$Hg NMR spectroscopy has become a powerful tool in this context due to the sensitivity of the $^{199}$Hg NMR shielding constants and chemical shifts to the first coordination sphere of Hg(II).[1–3]

Relativistic effects play an important role for NMR properties of systems containing heavy elements, such as mercury. From a computational point of view, there are several ways of treating relativistic effects. The first option is fully relativistic four-component linear response calculations[4] within program packages, such as DIRAC,[4–8] BERTHA,[9] MOLFDIR,[10] BDF,[11] and ReSpect.[12,13] A second option is computationally less demanding two-component methods, such as the zeroth-order regular approximation (ZORA),[14–18] exact two-component

methods,[19,20] Douglas-Kroll-Hess (DKH) approaches,[21–25] or the perturbational schemes by Melo *et al.*,[26,27] by Vaara *et al.*,[7,28,29] and the direct perturbation theory approach by Kutzelnigg.[30]

The first *ab initio* calculations including relativistic effects of $^{199}$Hg NMR shielding constants in mercury halides were presented by Nakatsuji *et al.*[31] They used a method which is a combination of a relativistic spin-free no-pair theory and the spin-orbit (SO) unrestricted Hartree-Fock (HF) method and concluded that spin-free terms, such as the mass-velocity and Darwin terms, and the spin-orbit term are important and that they strongly couple with each other. Moreover, they showed that for $^{199}$Hg NMR shielding constants and chemical shifts the spin-orbit term of the halogen becomes more important for the heavier halogens. This conclusion was also supported by the study of Fukuda *et al.*[24] who employed a method based on the DKH transformation. They also state that for more accurate predictions of the chemical shifts of these molecules one should consider electron correlation effects. Using ZORA at the density functional theory (DFT) level, Wolff *et al.*[18] showed that mercury NMR shielding

a)Electronic mail: vaida@life.ku.dk.

**135**, 044306-1

constants strongly depend on the structure of mercury halides. Finally, Taylor *et al.*[32] conducted recently a ZORA-DFT study on $^{199}$Hg NMR shielding constants of Hg(CH$_3$)$_2$, solid HgCl$_2$, and of HgCl$_2$ complexed with DMSO. To the best of our knowledge, four-component relativistic calculations of NMR shielding constants have not yet been presented for Hg(II) compounds, except that Fukuda *et al.*[23] employed the four-component/Dirac-Hartree-Fock (DHF) (Ref. 33) approach to calculate the $^{199}$Hg NMR shielding constant for Hg$^{78+}$ and Hg$^{70+}$ ions and Seino and Hada[25] employed a four-component scheme to calculate the NMR shielding constant of the Hg atom. On the other hand, four-component relativistic calculations of NMR shielding constants were performed for several other heavy metal compounds. Lantto *et al.*[7] have carried out DHF calculations on X$^{2+}$, X$^{4+}$, XH$_2$, and XH$_3^-$ (X = Si–Pb) as well as X$^{3+}$, XH$_3$, and XF$_3$ (X = P–Bi) systems and very recently Melo *et al.*[34] carried out DHF calculations on SnH$_2$XY and PbH$_2$XY (XY = F, Cl, Br, and I).

The goal of this study is thus (1) to compare the results of the approximate, two-component relativistic methods, linear response elimination of small component (LR-ESC) and ZORA, with results of fully relativistic four-component calculations of shielding constants and chemical shifts for linear-coordinated Hg(II) containing molecules, (2) to test convergence of the calculated shielding constants with basis set size, (3) to study the effect of using a Gaussian charge distribution model for the nuclear Coulomb potential as opposed to a point charge model, (4) to compare HF and DFT methods with different functionals, and finally (5) to compare the calculated Hg chemical shifts with experimental data. For that purpose we compare the performance of the three different relativistic methods (fully relativistic four-component calculations with the DIRAC program,[35,36] LR-ESC calculations with the DALTON code,[37] and ZORA calculations as implemented in the ADF program[38]) for the NMR shielding constants of all nuclei and the Hg chemical shifts in linear HgL$_2$ (L = Cl, Br, I, CH$_3$) compounds. Moreover, we investigate how much the choice of the common gauge origin (GO) and non-collinear spin-density contribution to the exchange-correlation (XC) kernel influence the outcome of the calculations.

## II. COMPUTATIONAL DETAILS

### A. Four-component calculations

Four-component fully relativistic shielding constant calculations with a common gauge origin for the vector potential were carried out using the DIRAC V.08 code[35] at the DHF and DFT levels. DIRAC V.10 version[36] was released during the revision of the paper and was employed for calculations using gauge-including atomic orbitals (GIAO) (Refs. 8 and 39) as well as for calculations with non-collinear spin density contribution to the XC kernel (non-collinear spin-magnetization). In addition to the hybrid B3LYP (Refs. 40 and 41) and PBE0 (Refs. 42–45) functionals, we employed the generalised gradient approximation (GGA) BP86 (Refs. 46 and 47) functional, which has been used previously in calculations of $^{199}$Hg NMR shielding constants in Ref. 32 and 48. The nuclear magnetic shielding constant was calculated as four-component linear response functions.[4] In order to re-

duce the computational cost, we performed approximate Dirac-Coulomb calculations, where the interatomic small component–small component (SS) integral contribution is modelled by the classical repulsion of small component atomic charges as proposed by Visscher.[49] In addition, we used the unrestricted kinetic balance (UKB) condition,[50] which in contrast to the restricted kinetic balance (RKB) condition[50] allows to modify the coupling towards the magnetic balance between the large and small components of the relativistic wave function. It was shown that UKB ensures convergence of nuclear magnetic shielding constants with smaller basis sets than using the RKB condition.[8,51–54] In order to properly describe NMR shielding constants we use basis sets which contain tight functions. For the Hg, Br, and I atoms we used the basis sets by Dyall[55,56] dyall.cvxz (x=2,3,4) and for Cl, C, and H – Dunning's cc-pCVXZ (X=D,T,Q) basis sets were used,[57,58] all in their completely uncontracted form. The threshold value for convergence in the error vector (electronic gradient) was set to 1.0D-7. The convergence of the shielding constants with the basis set is discussed in Sec. III.

Three other computational issues have been addressed. The first issue refers to the choice of gauge origin of the vector potential within the common gauge origin approach and to the comparison with GIAO results at the DHF level (using DIRAC V.10) and is discussed in Sec. III. In the common GO case, the gauge origin was placed at the heavy nucleus Hg when calculating $^{199}$Hg NMR shielding constants, whereas in calculations of NMR shielding constants of lighter nuclei (Cl, Br, I, C, H), the gauge origin was placed either at the position of the nucleus in question or at the Hg nucleus. The second issue concerns the choice of the nuclear charge model for the Coulomb potential of the nuclei. Here, we have used both a Gaussian charge distribution or a point charge model for the Coulomb potential, whereas in the expression for the vector potential of the nuclear magnetic moment, only a point nucleus model is available. Consequently, we introduce the following abbreviations, which are used throughout the paper. *p.p.* or point/point indicates that the point nucleus model has been used for both the Coulomb and vector potential of the nucleus, while *g.p.* or Gaussian/point implies that a Gaussian charge distribution was used for the Coulomb and a point nucleus model for the vector potential of the nuclear magnetic moment. The Gaussian charge distribution nuclear model is a more physical model to describe the nuclear charge distribution than the point charge model and we employ a Gaussian charge distribution with exponents proposed by Visscher and Dyall.[59] The results of this study are presented in Sec. IV. The last issue investigates how non-collinear spin-density contribution to the XC kernel changes the shielding constant and Hg chemical shift values in DFT calculations and is discussed in Sec. V.

### B. LR-ESC calculations

LR-ESC calculations were carried out using the DALTON V2.0 code[37] at HF and DFT/BP86 levels with the exception of the $\sigma$(DIA-K) contributions,[60] which are implemented in a local development version of DALTON V2.0. In

the LR-ESC scheme, the total relativistic nuclear magnetic shielding constant is calculated as the sum of the non-relativistic (NR) shielding constants and corrections according to the Rayleigh-Schrödinger perturbation theory expressions.[26, 27] Dyall's dyall.cvxz (x=2,3,4) basis sets were used for Hg, Br, I, whereas H, C, and Cl were described using Dunning's cc-pCVXZ (X=D,T,Q) basis sets, all in their uncontracted form. Employed basis sets had enough tight functions in order to obtain converged paramagnetic LR-ESC terms.[27, 60] A convergence threshold of 1.0D-06 for the energy gradient was used. The basis set convergence is discussed in Sec. III. Although it was previously shown that the LR-ESC scheme is gauge invariant in the limit of a complete basis set (CBS),[61] in actual calculations using a finite basis set gauge origin independence can only be achieved by special methods such as the distributed gauge origin methods GIAO, individual gauge for localized orbitals (IGLO),[62, 63] or continuous transformation of the origin of the current density (CTOCD).[64–66] As none of these have been implemented for the relativistic corrections in the LR-ESC approach, we have used GIAOs in the calculation of the non-relativistic shielding constants[67] and the common-origin approach with the gauge origin fixed at the position of each studied nucleus or other nucleus for the relativistic corrections in the LR-ESC approach which is more thoroughly discussed in Sec. III. Concerning the choice of nuclear charge model for the Coulomb potential of the nuclei in the LR-ESC scheme, which combines a non-relativistic shielding constant calculation with relativistic corrections to it, it is more consistent to use only the point nucleus model (*p.p.*) in both the non-relativistic and relativistic calculations. For the vector potential of the nuclear magnetic moment only the point nucleus model is available. Spin-density contribution in the LR-ESC-DFT scheme appears in the property calculation part through coupling of spin-dependent perturbation operators with perturbed states which may not have a zero spin.

### C. ZORA calculations

NMR shielding constants were also calculated with the ZORA approach.[14–17] All calculations were carried out using the NMR module[18, 68, 69] of the ADF v.2009.01 program[38] at the DFT level with the BP86, B3LYP, and PBE0 functionals. ZORA relativistic Slater type all-electron basis sets[70] were used in the form of GIAOs.[71–73] As recommended by ADF developers, for accurate hybrid calculations we added more diffuse fit functions and used the strict criteria for the basis set dependence, namely, bas = $1 \times 10^{-4}$. The threshold value for convergence in the error vector was set to 1.0D-8. In the ZORA calculations, as in the four-component calculations, we could choose between the Gaussian charge distribution and the point charge model for the Coulomb potential, but we had only the option of a point nucleus model for the vector potential of the nuclear magnetic moment. Thus, we performed *g.p.* and *p.p.* calculations.

Spin-orbit coupling is included variationally in the solution of the Kohn-Sham equations for the closed shell ground state. In the solution of the DFT response equations, necessary for the calculation of the shielding constants, the ex-

TABLE I. Experimental gas phase electron diffraction geometries of $HgL_2$ (L = Cl, Br, I, $CH_3$) compounds used in this study. Bond lengths are in Å and angles are in degrees.

| Molecule | Geometry |
|---|---|
| $HgCl_2$ | r(Hg–Cl) = 2.252 ± 0.005[a] |
| $HgBr_2$ | r(Hg–Br) = 2.41 ± 0.01[b] |
| $HgI_2$ | r(Hg–I) = 2.554 ± 0.003[c] |
| $Hg(CH_3)_2$ | r(Hg–C) = 2.083 ± 0.003[d] |
| | r(C–H) = 1.106 (assumed)[d] |
| | ∠(H–C–H) = 109.5 (assumed) |

[a]Geometry taken from Ref. 74.
[b]Geometry taken from Ref. 75.
[c]Geometry taken from Ref. 76.
[d]Geometry taken from Ref. 77.

ternal magnetic field perturbation leads to a first order spin-density and, consequently, to a Fermi-contact (-like) contribution to the NMR shielding constant, which is calculated in the ADF NMR calculation. However, the contribution to the DFT part of the exchange-correlation kernel of the response equations is neglected in ADF contrary to the four-component calculations with spin-density contribution to the XC kernel. Therefore, only uncoupled perturbed Kohn-Sham equations are solved for GGA or local-density approximation functionals in the ADF NMR calculations. In the case of hybrid functionals, such as B3LYP, the Hartree-Fock exchange potential leads furthermore to a first order change of the orbitals due to the external magnetic field, which makes it necessary to solve coupled perturbed Kohn-Sham equations, but the first order spin-density is still not taken into account in the DFT part of the exchange-correlation potential.[68, 69]

### D. Geometries of Hg compounds

NMR shielding constants were calculated for linear $HgL_2$ (L = Cl, Br, I, $CH_3$) compounds. We used experimental geometries (see Table I for details) obtained with electron diffraction in the gas phase.[74–77] For $Hg(CH_3)_2$ nearly free rotation of the methyl groups was reported;[77] therefore, the Hg–$CH_3$ bond-length (2.083 Å) was interpreted as the average configuration. We chose to test two different positions of methyl groups–with dihedral angle 0° in eclipsed structure and dihedral angle 60° in staggered structure, using ADF/ZORA approach. We obtained Hg NMR shielding constants: $\sigma(^{199}Hg)$ = 7929 ppm and $\sigma(^{199}Hg)$ = 7932 ppm for the eclipsed and staggered structures, respectively. Herein, we used the BP86 functional, the point/point nucleus models, and a TZ2P basis set. We conclude, that both conformations give virtually identical Hg shielding constants and both results are in a good agreement with the earlier result $\sigma(^{199}Hg)$ = 7929 ppm obtained by Taylor *et al.*[32] using ADF/ZORA with the same functional and basis set. In the following we will therefore only consider the eclipsed conformer.

### III. SELECTION OF BASIS SET AND GAUGE ORIGIN

We have investigated the basis set dependence of the shielding constants calculated with all three relativistic methods for the smallest halogen system $HgCl_2$. The

TABLE II. **Basis set dependence of four-component calculations**: shielding constants, $\sigma(^{199}\mathrm{Hg})$ and $\sigma(^{35}\mathrm{Cl})$, (in ppm) of $\mathrm{HgCl}_2$ as a function of different basis sets calculated using the four-component method at the Dirac-Hartree-Fock (DHF) and DFT/BP86 levels in combination with Gaussian/point nucleus models.

| | $\sigma(^{199}\mathrm{Hg})$ | | | $\sigma(^{35}\mathrm{Cl})$ | | | |
| | GIAO | GO=Hg | | GIAO | GO=Hg | | GO=Cl |
| Basis set Hg/Cl | DHF | DHF | DFT | DHF | DHF | DFT | DHF |
|---|---|---|---|---|---|---|---|
| dyall.cv2z/cc-pCVDZ | 13 600 | 13 732 | 12 203 | 1124 | 1194 | 894 | 884 |
| dyall.cv3z/cc-pCVTZ | 13 580 | 13 605 | 12 049 | 1126 | 1145 | 860 | 918 |
| dyall.cv4z/cc-pCVQZ | 13 613 | 13 618 | 12 049 | 1131 | 1137 | 856 | 947 |

four-component, LR-ESC, and ZORA results are presented in Tables II, III, and V, respectively.

In the four-component and LR-ESC calculations we have employed Dyall's[55,56] basis sets dyall.cv2z ($22s19p12d9f1g$), dyall.cv3z ($29s24p15d11f4g1h$), and dyall.cv4z ($34s30p19d13f4g2h$) for Hg and Dunning's[57,58] basis sets cc-pCVDZ ($13s9p2d$), cc-pCVTZ ($17s11p4d2f$), and cc-pCVQZ ($19s14p6d4f2g$) for Cl. Both series of basis sets are designed to converge systematically to the CBS limit of the total energy. Dunning's correlation consistent basis set has frequently also been used in extrapolation schemes for NMR shielding and spin-spin coupling constants.[78,79]

In Table II we present results of the basis set study for four-component calculations. The DHF gauge independent (GIAO) calculations give similar values of the NMR shielding constant, $\sigma(^{199}\mathrm{Hg})$, with all three basis sets, and thus appear to be converged to within 20 ppm already with the dyall.cv2z/cc-pCVDZ basis set. With the gauge origin placed at Hg the shielding constant changes only marginally between the two largest basis sets and thus also appears to be converged. This is further supported by the fact that the results converge towards those obtained with the GIAO method, displaying a difference of 132 ppm, 25 ppm, and 5 ppm with the dyall.cv2z/cc-pCVDZ, dyall.cv3z/cc-pCVTZ, and dyall.cv4z/cc-pCVQZ basis sets, respectively. Finally, at the DFT/BP86 level the dyall.cv3z/cc-pCVTZ and dyall.cv4z/cc-pCVQZ basis sets give the same Hg shielding constant value of 12 049 ppm, indicating that the dyall.cv3z/cc-pCVTZ basis set is already close to the CBS limit. Regarding the Cl NMR shielding constant, the trends are similar for the GIAO calculations and when the gauge origin is placed at Hg. However,

placing the gauge origin at Cl gives a significantly different shielding constant and poorer convergence. Consequently, in the following DHF and DFT calculations, we place the GO at Hg, and in order to save computational resources, we decided to use the dyall.cv3z basis set for Hg, Br, I and the cc-pCVTZ basis set for H, C, Cl in all further four-component calculations.

The results of a basis set study for the LR-ESC approach at the HF level are presented in Table III. We do not observe as good convergence for the Hg shielding constant as in the four-component calculations. The difference between the Hg shielding constant values obtained using dyall.cv3z/cc-pCVTZ and dyall.cv4z/cc-pCVQZ is about 5 times larger than going from dyall.cv2z/cc-pCVDZ to dyall.cv3z/cc-pCVTZ. Thus, this is a slight divergence of the LR-ESC results with increasing the basis set. The dyall.cv3z result for the Hg NMR shielding constant differs by 1.5% (150 ppm) from the dyall.cv4z/cc-pCVQZ result. For Cl, on the other hand, the difference amounts to only 0.5% (6 ppm). To put the remaining basis set errors into perspective, it is useful to compare this with the deviations from the four-component results with the same basis set, which amount to 23% (3091 ppm) for Hg and 2.5% (29 ppm) for Cl using the dyall.cv3z/cc-pCVTZ basis set. We consider thus that the remaining basis set error in the LR-ESC results for Hg is irrelevant compared to the one order of magnitude larger deviations

TABLE III. **Basis set dependence of LR-ESC calculations**: shielding constants, $\sigma(^{199}\mathrm{Hg})$ and $\sigma(^{35}\mathrm{Cl})$, (in ppm) of $\mathrm{HgCl}_2$ as a function of different basis sets calculated using the LR-ESC method at the HF level in combination with point/point nucleus models. The total relativistic nuclear magnetic shielding constant is calculated as the sum of non-relativistic shielding constants (obtained by GIAO) and corrections according to the Rayleigh-Schrödinger perturbation theory expressions (obtained by common gauge origin (GO)).

| Basis set | $\sigma(^{199}\mathrm{Hg})$ GO=Hg | $\sigma(^{35}\mathrm{Cl})$ GO=Cl |
|---|---|---|
| dyall.cv2z/cc-pCVDZ | 10 487 | 1054 |
| dyall.cv3z/cc-pCVTZ | 10 514 | 1173 |
| dyall.cv4z/cc-pCVQZ | 10 664 | 1179 |

TABLE IV. **The choice of gauge origin (GO) in LR-ESC**: shielding constants, $\sigma(N)$ ($N$ = Hg, C, Cl, Br, I), were calculated as the sum of non-relativistic shielding constants (obtained by GIAO) and LR-ESC corrections at the HF level in combination with point/point nucleus models and dyall.cv3z basis set for Hg, Br, I and cc-pCVTZ basis set for H, C, Cl. We calculated LR-ESC corrections using the common-origin approach with the GO fixed either at the position of each studied nucleus $N$ or fixed at the position of the other nucleus.

| Molecule | $N$ | NR GIAO | LR-ESC corrections GO=$N$ | GO=other | LR-ESC total GO=$N$ | GO=other |
|---|---|---|---|---|---|---|
| $\mathrm{Hg(CH_3)_2}$ | Hg | 6695.0 | 2755.7 | 2755.2 | 9450.7 | 9450.2 |
| $\mathrm{HgCl_2}$ | Hg | 7548.4 | 2965.6 | 2965.6 | 10 514.0 | 10 514.0 |
| $\mathrm{HgBr_2}$ | Hg | 7541.4 | 3100.0 | 3100.1 | 10 641.4 | 10 641.5 |
| $\mathrm{HgI_2}$ | Hg | 7177.1 | 3280.6 | 3280.8 | 10 457.7 | 10 457.9 |
| $\mathrm{Hg(CH_3)_2}$ | C | 217.8 | −42.6 | −35.9 | 175.2 | 181.9 |
| $\mathrm{HgCl_2}$ | Cl | 1201.7 | −28.5 | −27.3 | 1173.2 | 1174.4 |
| $\mathrm{HgBr_2}$ | Br | 3162.9 | 124.0 | 121.5 | 3286.9 | 3284.4 |
| $\mathrm{HgI_2}$ | I | 5455.8 | 735.6 | 733.4 | 6191.4 | 6189.2 |

TABLE V. **Basis set dependence of ZORA calculations**: shielding constants, $\sigma(^{199}\text{Hg})$ and $\sigma(^{35}\text{Cl})$, (in ppm) of $HgCl_2$ as a function of different basis sets calculated using the ZORA method at the DFT/BP86 level in combination with Gaussian/point nucleus models.

| Basis set | $\sigma(^{199}\text{Hg})$ GIAO | $\sigma(^{35}\text{Cl})$ GIAO |
|---|---|---|
| DZ | 9732 | 817 |
| TZ | 10 452 | 874 |
| TZP | 9606 | 853 |
| TZ2P | 9541 | 854 |
| QZ | 10 408 | 862 |
| QZ2P | 9957 | 837 |
| QZ4P | 9948 | 835 |

from the four-component results and that it has no significant impact on our conclusions concerning the performance of the LR-ESC method for the Hg shielding constants presented in this work. As we prefer to use in the LR-ESC calculations a basis set as similar to one of the four-component calculations as possible and because four-component calculations for the heavier systems using the dyall.cv4z/cc-pCVQZ basis set are too resource demanding, we will in all further LR-ESC calculations employ the dyall.cv3z for Hg, Br, I and cc-pCVTZ for H, C, Cl. We have also investigated the effect of moving the common gauge origin in the calculation of the relativistic corrections from the nucleus of interest to the other nucleus. The results of this study are presented in Table IV. LR-ESC corrections to the Hg shielding constant change by at most 0.5 ppm due to the change of gauge origin, whereas at most 2.5 ppm and 6.7 ppm differences are observed for halogen and C shielding constants, respectively. This confirms the results of a very recent study on the shielding constants in $SnH_2F_2$,[34] where a similarly small gauge origin dependence of LR-ESC results was observed. Due to the small gauge origin dependence of LR-ESC results, in the following calculations we place the gauge origin at the nucleus of interest only.

The results of the basis set study with the ZORA approach are given in Table V. We have used all the ZORA relativistic Slater type all-electron basis sets, which are provided by the ADF program for Hg and Cl: DZ ($13s10p6d3f/6s4p$), TZP ($14s10p7d3f/7s5p1d$), TZ2P ($14s10p7d4f/7s5p1d1f$), QZ4P ($22s18p12d6f/11s7p3d2f$) for Hg/Cl, respectively. In order to perform a thorough basis set convergence study, we additionally constructed TZ ($14s9p7d3f/7s5p$), QZ ($22s15p11d4f/11s7p$), and QZ2P ($22s17p12d5f/11s7p2d1f$) basis sets, by eliminating polarisation functions or replacing polarisation functions from the TZP and QZ4P basis sets with smaller number of functions with the average exponent (these basis sets are available as supplementary material[80]). Here, there appear to be two opposing basis set convergence patterns. First, in the DZ $\Rightarrow$ TZ $\Rightarrow$ QZ series the shielding constant varies as 9732 ppm $\Rightarrow$ 10 452 ppm $\Rightarrow$ 10 408 ppm. Thus, the TZ result differs by less than 50 ppm from the QZ result and there seems to be convergence to within this error in this series. When polarisation functions are added to the TZ and QZ basis sets, the Hg NMR shielding constant decreases (the same is observed for Cl NMR shielding constant) and appears to be converged to within 10 ppm in the series QZ

$\Rightarrow$ QZ2P $\Rightarrow$ QZ4P. One could expect that adding more polarisation functions to the TZ2P basis set would lead to further reduction. But it is not possible to verify this within this work due to technical difficulties arising when adding polarisation functions. As a consequence of the opposing trends the standard ADF basis sets, TZ2P and QZ4P, give quite different Hg NMR shielding constant results (9541 ppm and 9948 ppm, respectively). For Cl the trends are quite similar to those observed for Hg, although TZ2P and QZ4P give results which are closer (854 ppm and 835 ppm, respectively). In the following we will employ the largest possible basis set, QZ4P, which also contains the largest number of high-exponent functions, important for the calculation of shielding constants and especially the spin-orbit term.

## IV. SELECTION OF THE NUCLEAR CHARGE MODEL FOR THE COULOMB POTENTIAL

In this section the selection of the nuclear charge model for the Coulomb potential in four-component and ZORA calculations is described. A Gaussian charge distribution or a point charge model for the Coulomb potential are applied together with a point nucleus model for the vector potential of the nuclear magnetic moment using the nomenclature Gaussian/point (*g.p.*) and point/point (*p.p.*) in the tables. The outcome of this investigation at the level of DFT/BP86 is presented in Table VI. From this we deduce that using a finite nucleus for the Coulomb potential reduces the Hg shielding constants by $\sim$100–500 ppm (about 1%–3%). A similar study was conducted by Fukuda *et al.*[23] who compared the values of heavy ion (including $Hg^{70+}$ and $Hg^{78+}$) shielding constants obtained by point and Gaussian nucleus models for both the Coulomb and vector potential of the nuclear magnetic moment using DHF and a two-component quasirelativistic theory based on the DKH transformation. Their conclusion was that using a Gaussian nucleus model gives rise to a decrease of the Hg shielding constant values by $\sim$500 ppm compared to calculations using a point nucleus model for $Hg^{70+}$ and $Hg^{78+}$ ions. Interestingly, the chemical shift, $\delta(^{199}\text{Hg})$, is also affected by the choice of nuclear model. In the four-component calculations the change from a point nucleus to a Gaussian nucleus model is 10 ppm, 70 ppm, and 143 ppm for $HgCl_2$, $HgBr_2$, and $HgI_2$, respectively. That is, it depends on the atomic number Z of the coordinating atom. For the ZORA calculations the same series gives a difference of 1 ppm, 40 ppm, and 97 ppm, and thus recovers from 10% to 68% of the finite nucleus effect observed with the four-component method. It is noteworthy that the observed reductions in ZORA calculations can be linked to the changes in the spin-orbit term (data not shown), and this is in a good agreement with the statement that the finite nucleus model affects the hyperfine structures of heavy atoms.[81,82]

For the shielding constants of the lighter atoms the effect is negligible ($\sim$0–1 ppm) and for iodine the change of the shielding constant is 15 ppm using the four-component method.

In Sec. V, we will present four-component and ZORA results which are obtained using the Gaussian nucleus model for the Coulomb potential.

TABLE VI. **Nuclear charge model**: shielding constants, $\sigma(N)$ ($N$ = Hg, C, Cl, Br, I), and chemical shifts, $\delta(^{199}\text{Hg})$, of HgL$_2$ (L = CH$_3$, Cl, Br, I) compounds (in ppm) calculated using four-component and ZORA approaches in combination with DFT/BP86, point/point (*p.p.*), and Gaussian/point (*g.p.*) nuclear models for the Coulomb and vector potentials, respectively. The Hg chemical shift is calculated as $\delta(^{199}\text{Hg}_{\text{HgL}_2}) = (\sigma(^{199}\text{Hg}_{\text{Hg(CH}_3)_2}) - \sigma(^{199}\text{Hg}_{\text{HgL}_2}))/(1 - \sigma(^{199}\text{Hg}_{\text{Hg(CH}_3)_2}))$.

| | | $\sigma(N)$ | | | | $\delta(^{199}\text{Hg})$ | | | |
| | | ZORA | | Four-component | | ZORA | | Four-component | |
| Molecule | $N$ | *p.p.* | *g.p.* | *p.p.* | *g.p.* | *p.p.* | *g.p.* | *p.p.* | *g.p.* |
|---|---|---|---|---|---|---|---|---|---|
| Hg(CH$_3$)$_2$ | Hg | 8084 | 7967 | 10 299 | 10 015 | | | | |
| HgCl$_2$ | Hg | 10 063 | 9948 | 12 343 | 12 049 | −1995 | −1996 | −2065 | −2055 |
| HgBr$_2$ | Hg | 11 335 | 11 179 | 13 606 | 13 254 | −3277 | −3237 | −3341 | −3271 |
| HgI$_2$ | Hg | 12 397 | 12 185 | 14 689 | 14 265 | −4348 | −4251 | −4435 | −4292 |
| Hg(CH$_3$)$_2$ | C | 155 | 155 | 155 | 155 | | | | |
| HgCl$_2$ | Cl | 834 | 835 | 860 | 860 | | | | |
| HgBr$_2$ | Br | 2379 | 2381 | 2515 | 2516 | | | | |
| HgI$_2$ | I | 4694 | 4698 | 5212 | 5197 | | | | |

## V. RESULTS AND DISCUSSION

### A. Relativistic corrections to shielding constants and Hg chemical shifts

In this section, we compare the performance of three relativistic methods (four-component, LR-ESC, and ZORA) in calculations of NMR parameters of HgL$_2$ (L = CH$_3$, Cl, Br, I) compounds, and describe the magnitude of the relativistic correction (i.e., the difference of the shielding constant calculated with non-relativistic and relativistic methods). The calculations were performed at the level of HF and DFT theories. Regarding the latter, we employed three different functionals (GGA/BP86 and the hybrid functionals B3LYP and PBE0). In the upper part of Table VII, shielding constants, $\sigma(N)$ ($N$ = Hg, C, Cl, Br, I), are presented, whereas the bottom part of the table is dedicated to Hg chemical shifts, $\delta(^{199}\text{Hg})$.

The results of the DFT/BP86 calculations in Table VII illustrate that the relativistic corrections follow a systematic trend as a function of the atomic number of the nucleus in question. The differences between the four-component and non-relativistic results for the shielding constants of the ligand atoms increase from carbon (−41 ppm) over chlorine (−183 ppm) and bromine (−272 ppm) to iodine (+310 ppm). For carbon and probably chlorine this is due to the HALA effect (heavy atom effect on the shielding of a light atom) from the neighbouring Hg atom, whereas for bromine and iodine there are in addition HAHA effects[83] (heavy atom effects on the shielding of the heavy atom itself). At the same time also the relativistic correction to the Hg shielding constant increases with the atomic number of the ligand atom: 3893 ppm in Hg(CH$_3$)$_2$, 4846 ppm in HgCl$_2$, and finally 7474 ppm in HgI$_2$ as shown in Fig. 1(a) and can be attributed to HAVHA effect (heavy atom effect on vicinal heavy

TABLE VII. **Comparison of relativistic methods**: shielding constants, $\sigma(N)$ ($N$ = Hg, C, Cl, Br, I), and chemicals shifts, $\delta(^{199}\text{Hg})$, calculated using non-relativistic method (NR) (with GIAO) and three different relativistic methods: LR-ESC and four-component (without and with spin-density contribution to the XC kernel) using common gauge origin and ZORA using GIAO. The calculations were performed at the level of HF and DFT in combination with three different functionals BP86, B3LYP, and PBE0. The Hg chemical is calculated as $\delta(^{199}\text{Hg}_{\text{HgL}_2}) = (\sigma(^{199}\text{Hg}_{\text{Hg(CH}_3)_2}) - \sigma(^{199}\text{Hg}_{\text{HgL}_2}))/(1 - \sigma(^{199}\text{Hg}_{\text{Hg(CH}_3)_2}))$.

| | | | | | | | DFT | | | | | |
| | | | HF | | | | BP86 | | | B3LYP | | PBE0 |
| Molecule | $N$ | NR | LR-ESC | Four-component | NR | LR-ESC | ZORA | Four-component (spin-density) | ZORA | Four-component | ZORA | Four-component |
|---|---|---|---|---|---|---|---|---|---|---|---|---|
| | | | | | Shielding constants, $\sigma(N)$ ($N$ = Hg, C, Cl, Br, I) | | | | | | | |
| Hg(CH$_3$)$_2$ | Hg | 6695 | 9451 | 12 054 | 6122 | 8533 | 7967 | 10 015 (10 276) | 8326 | 10 381 | 8484 | 10 536 |
| HgCl$_2$ | Hg | 7548 | 10 514 | 13 605 | 7203 | 10 010 | 9948 | 12 049 (12 306) | 10 256 | 12 353 | 10 354 | 12 443 |
| HgBr$_2$ | Hg | 7541 | 10 641 | 14 636 | 7195 | 10 355 | 11 179 | 13 254 (13 691) | 11 450 | 13 528 | 11 454 | 13 526 |
| HgI$_2$ | Hg | 7177 | 10 458 | 15 686 | 6791 | 10 403 | 12 185 | 14 265 (14 845) | 12 473 | 14 561 | 12 407 | 14 496 |
| Hg(CH$_3$)$_2$ | C | 218 | 175 | 169 | 196 | 156 | 155 | 155 (150) | 156 | 156 | 164 | 164 |
| HgCl$_2$ | Cl | 1202 | 1173 | 1145 | 1043 | 938 | 835 | 860 (860) | 906 | 929 | 938 | 965 |
| HgBr$_2$ | Br | 3163 | 3287 | 3246 | 2788 | 2728 | 2381 | 2516 (2539) | 2549 | 2686 | 2651 | 2789 |
| HgI$_2$ | I | 5456 | 6191 | 6367 | 4887 | 5369 | 4698 | 5197 (5280) | 4959 | 5464 | 5133 | 5637 |
| | | | | | Chemical shifts, $\delta(^{199}\text{Hg})$ | | | | | | | |
| HgCl$_2$ | Hg | −859 | −1073 | −1570 | −1087 | −1489 | −1996 | −2055 (−2051) | −1946 | −1992 | −1886 | −1927 |
| HgBr$_2$ | Hg | −851 | −1201 | −2613 | −1079 | −1838 | −3237 | −3271 (−3450) | −3150 | −3180 | −2995 | −3021 |
| HgI$_2$ | Hg | −485 | −1017 | −3676 | −673 | −1886 | −4251 | −4292 (−4617) | −4181 | −4223 | −3956 | −4002 |
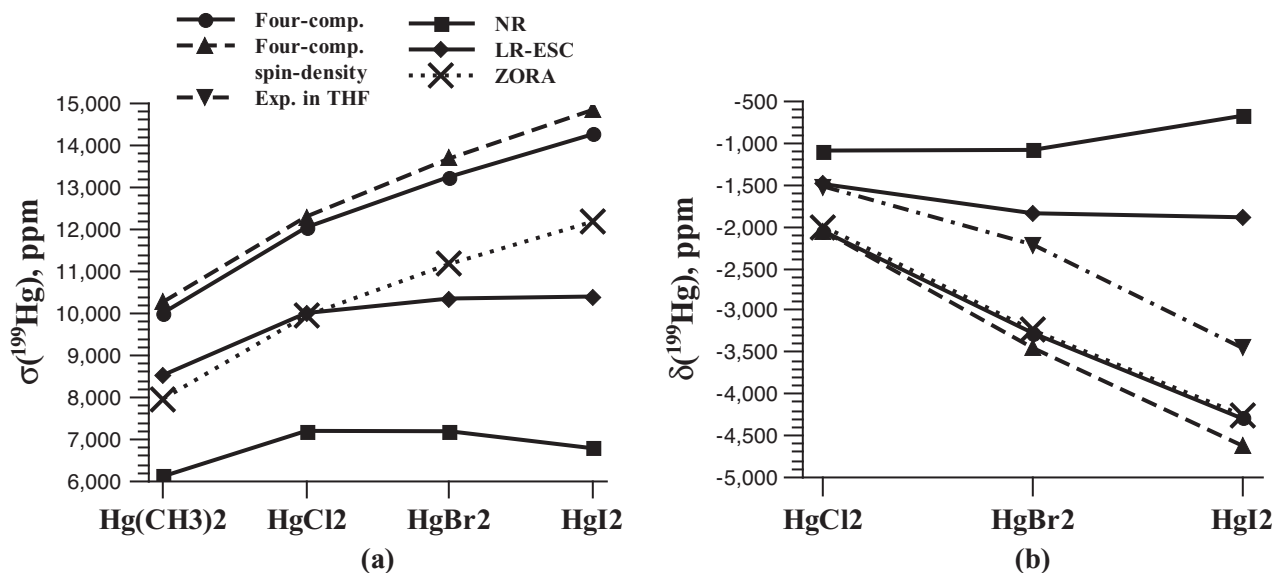
FIG. 1. (a) Shielding constants, $\sigma(^{199}Hg)$, and (b) chemical shifts, $\delta(^{199}Hg)$, of $HgL_2$ (L = CH$_3$, Cl, Br, I) compounds calculated using NR, LR-ESC, ZORA, and four-component methods at the DFT/BP86 level and determined experimentally in THF. All the calculated values are from Table VII and experimental values are from Table X.

atom).[34,54] These trends are repeated in the HF calculations; however, the relativistic effects are somewhat larger for mercury, such as 5359 ppm in $Hg(CH_3)_2$, 6057 ppm in $HgCl_2$, and finally 7095 ppm in $HgI_2$, whereas the shielding constant of the ligand atoms increases in absolute value from carbon (−49 ppm) over chlorine (−57 ppm) and bromine (+89 ppm) to iodine (+911 ppm). The relativistic corrections to the mercury chemical shifts are 968 ppm, 2192 ppm, and 3619 ppm for $HgCl_2$, $HgBr_2$, and $HgI_2$, respectively, at the level of DFT/BP86. This follows the normal halogen dependence[84,85] behaviour in which an increased spin-orbit contribution is found for the heavier halogen ligands .[18,24,31]

In the following paragraph the performance of the two-component methods is discussed (see also Fig. 1). For the C shielding constant, both LR-ESC and ZORA reproduce the relativistic corrections of four-component calculations. For Cl and Br, LR-ESC and ZORA behave differently: LR-ESC underestimates relativistic corrections, whereas ZORA overestimates the relativistic corrections to the shielding constants. While for I (which is also considered as heavy atom besides Hg), LR-ESC overestimates relativistic corrections and ZORA calculations even give the incorrect sign of the relativistic correction. It has previously been reported that ZORA might give errors for heavy atom properties that depend on the core orbitals, such as absolute shielding constants, whereas chemical shifts are reproduced well, *vide infra*.[86] For Hg shielding constants, LR-ESC predicts relativistic corrections of 2411 ppm, 2807 ppm, 3160 ppm, and 3612 ppm for $Hg(CH_3)_2$, $HgCl_2$, $HgBr_2$, and $HgI_2$, accordingly, which in percentage amounts to ∼58% ⇒ 45% of the total relativistic corrections for the $Hg(CH_3)_2$⇒$HgI_2$ series at the DFT/BP86 level. ZORA estimates relativistic corrections of 1845 ppm, 2745 ppm, 3984 ppm, and 5394 ppm for $Hg(CH_3)_2$, $HgCl_2$, $HgBr_2$ and $HgI_2$, accordingly, which in percentage amounts to ∼47% ⇒ 72% of the total relativistic corrections. However, even though

ZORA underestimates Hg NMR shielding constants by ∼2100 ppm, the differences between Hg chemical shift values obtained using ZORA and four-component approaches (without spin-density contribution to the XC kernel) are less than 60 ppm and are similar for all three compounds as shown in Table VII and Fig. 1. This is in a good agreement with the conclusion made by Autschbach[86] that ZORA is a reliable tool for the investigation of chemical shifts as a "valence" property due to very accurate hyperfine integrals for the valence shells of heavy atoms in contrast to inner-most core shells which are important for shielding constants.

In order to evaluate SO contribution to Hg shielding constants and chemical shifts in $HgL_2$ (L = Cl, Br, I) compounds and understand why LR-ESC does not reproduce the Hg chemical shift trend with increasingly heavy halogen ligands, we determined the SO terms in the Hg shielding constants of $HgL_2$ (L = CH$_3$, Cl, Br, I) compounds obtained by four-component,[4] LR-ESC,[27] and ZORA (Ref. 18) methods in combination with DFT/BP86 (see Table VIII). Since these methods define the SO terms differently, the direct comparison of SO terms is not possible. Therefore, we present for the $HgL_2$ (L = Cl, Br, I) compounds also the changes from the total Hg shielding constant and SO term values in $Hg(CH_3)_2$ (see Table VIII in parenthesis). For $HgCl_2$, the change in the SO term (463 ppm), obtained with the four-component approach without spin-density contribution to the XC kernel, corresponds to 23% of the change in total Hg shielding constant value. LR-ESC yields a change of 154 ppm in the SO term and therefore reproduces 33% of the change in SO term obtained with the four-component approach without spin-density contribution to the XC kernel. This underestimation of the change in the SO term accounts for 55% of the difference in the change of the total Hg shielding constant value. The change in SO terms and the contribution to the change in the total Hg shielding constant increases for $HgBr_2$

TABLE VIII. SO terms and the total values of Hg shielding constants of HgL$_2$ (L = CH$_3$, Cl, Br, I) compounds (in ppm) calculated using LR-ESC, ZORA, and four-component approaches (without and with spin-density contribution to the XC kernel) in combination with DFT/BP86. In parenthesis we present the changes from the total Hg shielding constant and SO term values in Hg(CH$_3$)$_2$. The SO term in the four-component approach (without and with spin-density contribution to the XC kernel) was calculated as the difference between Hg shielding constant value calculated including SO contribution and Hg shielding constant value calculated using spin-free formalism.

| Molecule | N | LR-ESC | | ZORA | | Four-component | | Four-component spin-density | |
|---|---|---|---|---|---|---|---|---|---|
| | | SO | Total | SO | Total | SO | Total | SO | Total |
| Hg(CH$_3$)$_2$ | Hg | −434 | 8533 | 2906 | 7967 | −1197 | 10 015 | −953 | 10 276 |
| HgCl$_2$ | Hg | −280 (154) | 10 010 (1477) | 3217 (311) | 9948 (1981) | −734 (463) | 12 049 (2034) | −494 (459) | 12 306 (2030) |
| HgBr$_2$ | Hg | 19 (453) | 10 355 (1822) | 4410 (1504) | 11 179 (3212) | 387 (1584) | 13 254 (3239) | 806 (1759) | 13 691 (3415) |
| HgI$_2$ | Hg | 467 (901) | 10403 (1870) | 5882 (2976) | 12 185 (4218) | 1743 (2940) | 14 265 (4250) | 2305 (3258) | 14 845 (4569) |

(1584 ppm and 49%) and even more for HgI$_2$ (2940 ppm and 69%) when using the four-component method without spin-density contribution to the XC kernel. Here, ZORA yields a very similar trend with 1504 ppm and 47% for HgBr$_2$ and 2976 ppm and 71% for HgI$_2$. For HgBr$_2$, ZORA reproduces 95% of the change in SO term obtained with the four-component approach without spin-density contribution to the XC kernel, whereas for HgI$_2$ it overestimates it by ∼1.2%. Therefore, the differences between Hg chemical shift values obtained using the ZORA and four-component approaches without spin-density contribution to the XC kernel are less than 60 ppm for all compounds, whereas LR-ESC underestimates the change in the SO term (453 ppm and 901 ppm) and reproduces only 29% and 31% of the change in SO term obtained with the four-component approach without spin-density contribution to the XC kernel for HgBr$_2$ and HgI$_2$, respectively. The underestimation of the change in SO term accounts for 80% and 86% of the difference in the change of the total Hg shielding constant value for HgBr$_2$ and HgI$_2$, respectively. Consequently, one can conclude that underestimation of the SO term is one of the main reasons why LR-ESC does not reproduce the trend in the Hg chemical shifts with increasingly heavy halogen ligands, but it is not the only reason.

All the DFT based four-component results discussed so far did not include spin-density contributions to the XC kernel in the calculations of the shielding constant. The impact of non-collinear spin-density contribution to the XC kernel on $\sigma(N)$ ($N$ = Hg, C, Cl, Br, I) shielding constants and $\delta(^{199}$Hg) chemical shifts in fully relativistic four-component calculations at the level of DFT/BP86 is presented in Table VII, in parenthesis under *(spin-density)* and in Fig. 1 as *Four-component spin-density*. While the C shielding constant is reduced by 5 ppm (3%) due to the non-collinear spin-density contribution, Cl shielding constant remains unaffected and Br and I shielding constants increase by 23 ppm (0.9%) and 81 ppm (1.5%), respectively. Within the series of halogen compounds, including non-collinear spin-density contribution gives rise to an increase of the Hg shielding constants and chemical shifts. Hg shielding constant values are increased by 261 ppm (2.6%), 257 ppm (2.1%), 437 ppm (3.3%), and 1581 ppm (4.1%) for Hg(CH$_3$)$_2$, HgCl$_2$, HgBr$_2$, and HgI$_2$, respectively. These changes are primarily due to the changes in SO terms as shown in Table VIII. Whereas Hg chemical shift in HgCl$_2$

is almost unaffected by non-collinear spin-density contribution (non-collinear spin-density effects on Hg shielding constants of Hg(CH$_3$)$_2$ and HgCl$_2$ cancel out), Hg chemical shifts in the heavier halogen compounds HgBr$_2$ and HgI$_2$ are reduced by 179 ppm (5.5%) and 325 ppm (7.5%). From this we conclude that Hg chemical shifts determined by the ZORA method agree very well with four-component/spin-density results for HgCl$_2$, whereas larger deviations (up to 366 ppm) occur for Hg chemical shifts in HgBr$_2$ and HgI$_2$.

### B. HF versus DFT

In this section results from HF calculations are compared with DFT calculations using three different functionals, GGA/BP86 and hybrids B3LYP (20% HF exchange) and PBE0 (25% HF exchange). In general, DFT reduces the shielding constants of all atoms and Hg chemical shifts compared to HF in LR-ESC and four-component calculations. The conclusion that DFT gives lower shielding constants compared to HF has been reported previously (e.g., in Ref. 87–90). In addition, hybrid functionals containing exact HF exchange lead to smaller reductions compared to GGA/BP86 and therefore give results which are in better agreement with HF, especially PBE0 which has a larger percentage of HF exchange than B3LYP. Furthermore, we observe that the differences between HF and DFT results increase with a more accurate treatment of relativistic corrections. The largest differences are thus observed in the four-component calculations. Finally, the calculated Hg chemical shifts using different functionals are similar in four-component and ZORA calculations.

### C. Shielding tensor elements and their relation to molecular structure and charge distribution

Obviously the isotropic shielding does not describe differences in individual tensor elements, nor differences between individual elements in a series of coordination compounds. Thus, it is conceivable that the same isotropic shielding is observed for two different molecules, despite the fact that the individual tensor elements are quite different, although this is not the case for the linear molecules investigated in this work. In Table IX the full shielding tensor in terms of components parallel and perpendicular to the molecular symmetry axis is presented for the four test

TABLE IX. Components of the total Hg shielding tensor (perpendicular $\sigma_\perp(^{199}Hg)$ and parallel $\sigma_\parallel(^{199}Hg)$ to the molecular symmetry axis) and isotropic shielding constants $\sigma(^{199}Hg)$ calculated with the four-component approach at the level of DFT/BP86 including non-collinear spin-density contribution to the XC kernel and with the gauge origin placed at Hg.

| Molecule | $\sigma_\perp(^{199}Hg)$ | $\sigma_\parallel(^{199}Hg)$ | $\sigma(^{199}Hg)$ |
|---|---|---|---|
| Hg(II) | 16 053 | 16 053 | 16 053 |
| Hg(CH$_3$)$_2$ | 7167 | 16 492 | 10 276 |
| HgCl$_2$ | 10 381 | 16 157 | 12 306 |
| HgBr$_2$ | 12 473 | 16 128 | 13 691 |
| HgI$_2$ | 14 483 | 15 569 | 14 845 |

molecules. As expected for a linear molecule, the anisotropy, i.e., the difference between the parallel and the perpendicular component, is high for Hg(CH$_3$)$_2$. The anisotropy decreases down the series HgCl$_2$ → HgBr$_2$ → HgI$_2$. This correlates with the molecular electric quadrupole moment (see Table II in supplementary material[80]), which is small for HgI$_2$, indicating that the charge distribution for this molecule is almost spherical. As such, this series of test molecules covers three important features of mercury containing compounds: (1) a systematic change from linear to almost spherical charge density, (2) a systematic increase in the atomic number of the ligand, and (3) both ionic and covalent Hg-ligand bonds are represented. Thus, the results presented in this work might be transferable to a broader selection of mercury containing molecules.

It is noteworthy that the parallel component of the shielding tensor is almost the same as that determined for Hg(II) ion. In a simple picture, this may be understood as the external magnetic field inducing a current around the symmetry axis of the molecule, which is similar to that induced in Hg(II) ion, whereas the induced current in the plane in which the co-

ordinating atom lies is hindered, leading to smaller values of the shielding tensor.

## D. Comparison with experimental data and other theoretical studies

In Table X other theoretical studies as well as experimental data are compiled for the four test molecules. Comparing the results in this work (four-component and ZORA) with the experimental data, the qualitative trends are the same, but there are large systematic quantitative differences amounting to up to ∼1000 ppm. These differences are even larger if we include the non-collinear spin-density contribution to the XC kernel in the four-component calculations. The use of hybrid functionals, B3LYP and especially PBE0, gives larger Hg chemical shift values by up to ∼300 ppm compared to the GGA/BP86 functional, and therefore, results in better correspondence with the experimental values. The differences between calculated and experimental values are expected because (1) rovibrational effects on the shielding constant are not included in the calculation, and probably more importantly, (2) the calculations are carried out in the gas phase, whereas the experiments are carried out in various solvents.[91–93] The linear geometries of mercury compounds were determined with electron diffraction studies in the gas phase and it was shown that they are bent in solution as the halide–Hg–halide bond angle decreases, as one chooses solvents with higher ability to coordinate to mercury.[94,95] For example, in DMSO the halide–Hg–halide angle was determined to be 162°, 158°, and 156° with Hg–halide bond distances 2.32 Å, 2.455 Å, and 2.625 Å (Ref. 96) for HgCl$_2$, HgBr$_2$, and HgI$_2$, respectively. Consequently, the coordination of solvent molecules to mercury changes the chemical shifts, $\delta(^{199}Hg)$.[91,92] Wolff et al.[18] showed that a change in 0.01 Å in bond-length leads to ∼50 ppm change in calculated

TABLE X. Shielding constants, $\sigma(Hg)$, and chemical shifts, $\delta(^{199}Hg)$, of HgL$_2$ (L = CH$_3$, Cl, Br, I) compounds (in ppm) reported in the literature are compared to values calculated in this work. The Hg chemical shift is calculated as $\delta(^{199}Hg_{HgL_2}) = (\sigma(^{199}Hg_{Hg(CH_3)_2}) - \sigma(^{199}Hg_{HgL_2}))/(1 - \sigma(^{199}Hg_{Hg(CH_3)_2}))$, with shielding constants obtained in this work, ZORA (Ref. 18) and FP-QR (Ref. 24) studies.

| | Calculated | | | | | | | | Experimental[a] | | | |
|---|---|---|---|---|---|---|---|---|---|---|---|---|
| | Four-component spin-density | Four-component | | | ZORA | ZORA[b] | SO-UHF[c] | FP-QR[d] | Water | THF | DMSO | Pyridine |
| Molecule | BP86 | BP86 | B3LYP | PBE0 | BP86 | Ref. [18] | Ref. [31] | Ref. [24] | Ref. [93] | Ref. [92] | Ref. [92] | Ref. [92] |
| | | | | | Shielding constants, $\sigma(^{199}Hg)$ | | | | | | | |
| Hg(CH$_3$)$_2$ | 10 276 | 10 015 | 10 381 | 10 536 | 7967 | 8019.9 | | 12 772.2 | | | | |
| HgCl$_2$ | 12 306 | 12 049 | 12 353 | 12 443 | 9948 | 9575.9 | 10 908 | 13 940.0 | | | | |
| HgBr$_2$ | 13 691 | 13 254 | 13 528 | 13 526 | 11 179 | 10 704.4 | 13 523 | 16 234.3 | | | | |
| HgI$_2$ | 14 845 | 14 265 | 14 561 | 14 496 | 12 185 | 11 526.0 | 14 943 | 17 551.6 | | | | |
| | | | | | Chemical shifts, $\delta(^{199}Hg)$ | | | | | | | |
| HgCl$_2$ | −2051 | −2055 | −1992 | −1927 | −1996 | −1568.5 | | −1182.9 | −1590.0 | −1518.6 | −1498.8 | −1279.5 |
| HgBr$_2$ | −3450 | −3271 | −3180 | −3021 | −3237 | −2706.2 | | −3506.8 | | −2213.1 | −2062.1 | −1622.2 |
| HgI$_2$ | −4617 | −4292 | −4223 | −4002 | −4251 | −3534.4 | | −4841.2 | | −3447.0 | −3119.0 | −2355.1 |

[a]Experimental $\delta(^{199}Hg)$ chemical shift values were determined in water, THF, DMSO, and pyridine.
[b]ZORA results are obtained by Wolff et al. (Ref. 18) using ADF package, PW91 functional, and TZ2P basis set with frozen cores.
[c]SO-UHF represents a combination of relativistic spin-free no-pair theory of Sucher and Hess and the spin-orbit unrestricted HF, which was employed by Nakatsuji et al. (Ref. 31). The results presented here were obtained using a relativistic hamiltonian (free particle) including spin-orbit effects.
[d]FP-QR (full name: GIAO-FP-QR-GUHF) method stands for the GIAO method for the finite perturbation theory and the GUHF wave function in combination with the QR-2 approximation was employed by Fukuda et al. (Ref. 24).

Hg chemical shift of $HgCl_2$, whereas every $10°$ change in Cl–Hg–Cl angle results in 100 ppm change of Hg chemical shift. According to the experiments from Refs. [93–95], the coordinating ability increases in the order water $\simeq$ THF < DMSO < pyridine. This is in good correspondence with the series we observe in Table X. The mercury chemical shifts obtained in the four-component and ZORA calculations are closest to experimental shifts in water and THF and deviate the most from the chemical shifts in pyridine.

Table X also lists the results obtained by other computational studies, such as ZORA by Wolff *et al.*,[18] SO-UHF by Nakatsuji *et al.*,[31] and GIAO-Finite Perturbation-quasirelativistic-generalized unrestricted Hartree-Fock (GIAO-FP-QR-GUHF) by Fukuda *et al.*[24] The ZORA calculations reported in Wolff *et al.* differ in several aspects from those presented in this work, such as DFT functional (BP86 versus PW91, which does not have a big influence: changes of 2-19 ppm for the Hg shielding constant in all four compounds were calculated using the QZ4P basis set and Gaussian/point nucleus models), and more notably different basis sets (QZ4P all-electron versus TZ2P frozen core). As demonstrated in Sec. III, using the TZ2P basis set, in contrast to QZ4P, gives an error of $\sim$400 ppm for Hg shielding constant in $HgCl_2$, accounting for most of the differences between the results of Wolff *et al.*[18] and the results presented in this work. Since TZ2P and QZ4P basis sets give similar Hg shielding constant values in $Hg(CH_3)_2$, contrary to $HgCl_2$, $HgBr_2$, and $HgI_2$, Hg chemical shifts are also affected by the choice of the basis set by $\sim$500 ppm (data not shown). Thus, despite the fact that the results of Wolff *et al.* for the Hg chemical shifts are in better correspondence with experimental shifts, this agreement is probably accidental. Moreover, our ZORA results obtained with the QZ4P basis set are in much better agreement with four-component results.

## VI. CONCLUSIONS

We have presented a study of the performance of three different relativistic methods in the calculation of NMR shielding constants and Hg chemical shifts in linear $HgL_2$ (L = Cl, Br, I, $CH_3$) compounds. We find that for the C shielding constant both LR-ESC and ZORA reproduce the relativistic corrections and, therefore, the absolute value of the shielding constant obtained by the four-component approach. For Cl and Br these methods behave differently: LR-ESC underestimates the relativistic corrections, whereas ZORA overestimates the relativistic corrections to the shielding constants. For iodine LR-ESC overestimates relativistic corrections, while ZORA even gives the incorrect sign of the relativistic correction. Even though none of the two two-component methods, LR-ESC and ZORA, can reproduce relativistic corrections to the absolute shielding constants of mercury, ZORA reproduces the trend of relative relativistic corrections to the Hg shielding constant increasing with the atomic number of the ligand atom, contrary to LR-ESC, partly because the latter underestimates the change in spin-orbit contribution. The differences between Hg chemical shift values obtained using

ZORA and four-component approaches without spin-density contribution to the XC kernel are less than 60 ppm for all compounds using three different functionals, BP86, B3LYP, and PBE0. However, this difference increases up to 213 ppm and 366 ppm for $HgBr_2$ and $HgI_2$, respectively, if we compare with four-component calculations with non-collinear spin-density contribution to the XC kernel. However, we have investigated only linear mercury compounds and further studies would be necessary in order to test more generally that ZORA can be used as an alternative to the computationally demanding four-component approach for calculations of heavy atom chemical shifts. We have also shown that DFT reduces the shielding constants of all atoms and Hg chemical shifts compared to HF in LR-ESC and four-component calculations. It is noteworthy that hybrid functionals (B3LYP and PBE0) containing HF exchange lead to smaller reductions compared to GGA/BP86 and, therefore, results in better agreement with HF results. We have also found that the four-component method exhibits better basis set convergence than ZORA and LR-ESC methods. Moreover, we have investigated the effect on the Hg shielding constants and Hg chemical shifts of using a finite nucleus model in the form of a Gaussian charge distribution for the Coulomb potential of the nuclei and found that the effect is larger in four-component calculations compared to ZORA and increases with the atomic number of the coordinating atom.

[1]L. M. Utschig, J. W. Bryson, and T. V. O'Halloran, Science **268**, 380 (1995).
[2]O. Iranzo, P. W. Thulstrup, S. Ryu, L. Hemmingsen, and V. L. Pecoraro, Chem. Eur. J. **13**, 9178 (2007).
[3]M. Łuczkowski, M. Stachura, V. Schirf, B. Demeler, L. Hemmingsen, and V. L. Pecoraro, Inorg. Chem. **47**, 10875 (2008).
[4]L. Visscher, T. Enevoldsen, T. Saue, H. J. Aa. Jensen, and J. Oddershede, J. Comput. Chem. **20**, 1262 (1999).
[5]S. S. Gomez, R. H. Romero, and G. A. Aucar, J. Chem. Phys. **117**, 7942 (2002).
[6]J. Vaara and P. Pyykkö, J. Chem. Phys. **118**, 2973 (2003).
[7]P. Lantto, R. H. Romero, S. S. Gomez, G. A. Aucar, and J. Vaara, J. Chem. Phys. **125**, 184113 (2006).
[8]M. Iliaš, T. Saue, T. Enevoldsen, and H. J. Aa. Jensen, J. Chem. Phys. **131**, 124119 (2009).
[9]I. P. Grant and H. M. Quiney, Int. J. Quantum Chem. **80**, 283 (2000).
[10]L. Visscher, O. Visser, P. J.C. Aerts, H. Merenga, and W. C. Nieuwpoort, Comput. Phys. Commun. **81**, 120 (1994).

[11] L. Cheng, Y. Xiao, and W. Liu, J. Chem. Phys. **131**, 244113 (2009).

[12] S. Komorovský, M. Repiský, O. L. Malkina, V. G. Malkin, I. M. Ondik, and M. Kaupp, J. Chem. Phys. **128**, 104101 (2008).

[13] S. Komorovský, M. Repiský, O. L. Malkina, and V. G. Malkin, J. Chem. Phys. **132**, 154101 (2010).

[14] C. Chang, M. Pelissier, and P. Durand, Phys. Scr. **34**, 394 (1986).

[15] E. van Lenthe, E. J. Baerends, and J. G. Snijders, J. Chem. Phys. **99**, 4597 (1993).

[16] E. van Lenthe, E. J. Baerends, and J. G. Snijders, J. Chem. Phys. **101**, 9783 (1994).

[17] E. van Lenthe, J. G. Snijders, and E. J. Baerends, J. Chem. Phys. **105**, 6505 (1996).

[18] S. K. Wolff, T. Ziegler, E. van Lenthe, and E. J. Baerends, J. Chem. Phys. **110**, 7689 (1999).

[19] M. Iliaš and T. Saue, J. Chem. Phys. **126**, 064102 (2007).

[20] Q. Sun, W. Liu, Y. Xiao, and L. Cheng, J. Chem. Phys. **131**, 081101 (2009).

[21] K. Kudo and H. Fukui, J. Chem. Phys. **123**, 114102 (2005).

[22] K. Kudo and H. Fukui, J. Chem. Phys. **124**, 209901 (2006).

[23] R. Fukuda, M. Hada, and H. Nakatsuji, J. Chem. Phys. **118**, 1015 (2003).

[24] R. Fukuda, M. Hada, and H. Nakatsuji, J. Chem. Phys. **118**, 1027 (2003).

[25] J. Seino and M. Hada, J. Chem. Phys. **132**, 174105 (2010).

[26] J. I. Melo, M. C. Ruiz de Azua, C. G. Giribet, G. A. Aucar, and R. H. Romero, J. Chem. Phys. **118**, 471 (2003).

[27] J. I. Melo, M. C. Ruiz de Azua, C. G. Giribet, G. A. Aucar, and P. F. Provasi, J. Chem. Phys. **121**, 6798 (2004).

[28] P. Manninen, K. Ruud, P. Lantto, and J. Vaara, J. Chem. Phys. **122**, 114107 (2005).

[29] P. Manninen, K. Ruud, P. Lantto, and J. Vaara, J. Chem. Phys. **124**, 149901 (2006).

[30] W. Kutzelnigg, J. Comput. Chem. **20**, 1199 (1999).

[31] H. Nakatsuji, M. Hada, H. Kaneko, and C. C. Ballard, Chem. Phys. Lett. **255**, 195 (1996).

[32] R. E. Taylor, C. T. Carver, R. E. Larsen, O. Dmitrenko, S. Bai, and C. Dybowski, J. Mol. Struct. **930**, 99 (2009).

[33] Y. Ishikawa, T. Nakajima, M. Hada, and H. Nakatsuji, Chem. Phys. Lett. **283**, 119 (1998).

[34] J. I. Melo, A. Maldonado, and G. A. Aucar, Theor. Chem. Acc. **129**, 483 (2011).

[35] DIRAC, a relativistic *ab initio* electronic structure program, Release DIRAC08 (2008), written by L. Visscher, H. J. Aa. Jensen, and T. Saue, with new contributions from R. Bast, S. Dubbilard, K. G. Dyall, U. Ekström, E. Eliav, T. Fleig, A. S. P. Gomes, T. U. Helgaker, J. Henriksson, M. Iliaš, Ch. R. Jacob, S. Knecht, P. Norman, J. Olsen, M. Pernpointner, K. Ruud, P. Sałek, and J. Sikkema (see http://dirac.chem.sdu.dk).

[36] DIRAC, a relativistic *ab initio* electronic structure program, Release DIRAC10 (2010), written by T. Saue, L. Visscher, and H. J. Aa. Jensen, with contributions from R. Bast, K. G. Dyall, U. Ekström, E. Eliav, T. Enevoldsen, T. Fleig, A. S. P. Gomes, J. Henriksson, M. Iliaš, Ch. R. Jacob, S. Knecht, H. S. Nataraj, P. Norman, J. Olsen, M. Pernpointner, K. Ruud, B. Schimmelpfennig, J. Sikkema, A. Thorvaldsen, J. Thyssen, S. Villaume, and S. Yamamoto (see http://dirac.chem.vu.nl).

[37] DALTON, an *ab initio* electronic structure program, Release 2.0 (2005), see http://www.daltonprogram.org/.

[38] Amsterdam Density Functional ADF, Release ADF 2009.01 (2009), written by E. J. Baerends, B. te Velde, and collaborators (Amsterdam) and A. Rauk, T. Ziegler, and collaborators (Calgary) (see http://www.scm.com).

[39] A. E. Hansen and T. D. Bouman, J. Chem. Phys. **82**, 5035 (1985).

[40] P. J. Stephens, F. J. Devlin, C. F. Chabalowski, and M. J. Frisch, J. Phys. Chem. **98**, 11623 (1994).

[41] A. D. Becke, J. Chem. Phys. **98**, 5648 (1993).

[42] J. P. Perdew, K. Burke, and M. Ernzerhof, Phys. Rev. Lett. **77**, 3865 (1996).

[43] J. P. Perdew, K. Burke, and M. Ernzerhof, Phys. Rev. Lett. **78**, 1396 (1996).

[44] J. P. Perdew, K. Burke, and Y. Wang, Phys. Rev. B **54**, 16533 (1996).

[45] C. Adamo and V. J. Barone, J. Chem. Phys. **100**, 6158 (1999).

[46] A. D. Becke, Phys. Rev. A **38**, 3098 (1988).

[47] J. P. Perdew, Phys. Rev. B **33**, 8822 (1986).

[48] J. Jokisaari, S. Järvinen, J. Autschbach, and T. Ziegler, J. Chem. Phys. A **106**, 9313 (2002).

[49] L. Visscher, Theor. Chem. Acc. **98**, 68 (1997).

[50] K. G. Dyall and K. Fægri, Jr., Chem. Phys. Lett. **174**, 25 (1990).

[51] R. E. Stanton and S. Havriliak, J. Chem. Phys. **81**, 1910 (1984).

[52] M. Pecul, T. Saue, K. Ruud, and A. Rizzo, J. Chem. Phys. **121**, 3051 (2004).

[53] L. Visscher, Adv. Quantum Chem. **48**, 369 (2005).

[54] A. F. Maldonado and G. A. Aucar, Phys. Chem. Chem. Phys. **11**, 5615 (2009).

[55] K. G. Dyall, Theor. Chem. Acc. **112**, 403 (2004).

[56] K. G. Dyall, Theor. Chem. Acc. **115**, 441 (2006).

[57] D. E. Woon and T. H. Dunning, Jr., J. Chem. Phys. **98**, 1358 (1993).

[58] T. H. Dunning, Jr., J. Chem. Phys. **90**, 1007 (1989).

[59] L. Visscher and K. G. Dyall, At. Data Nucl. Data Tables **67**, 207 (1997).

[60] M. C. Ruiz de Azua, J. I. Melo, and C. G. Giribet, Mol. Phys. **101**, 3103 (2003).

[61] D. G. Zaccari, M. C. Ruiz de Azua, J. I. Melo, and C. G. Giribet, J. Chem. Phys. **124**, 054103 (2006).

[62] M. Schindler and W. Kutzelnigg, J. Chem. Phys. **76**, 1919 (1982).

[63] C. van Wüllen and W. Kutzelnigg, J. Chem. Phys. **104**, 2330 (1996).

[64] P. Lazzeretti, M. Malagoli, and R. Zanasi, Chem. Phys. Lett. **220**, 299 (1994).

[65] A. Ligabue, S. P. A. Sauer, and P. Lazzeretti, J. Chem. Phys. **118**, 6830 (2003).

[66] A. Ligabue, S. P. A. Sauer, and P. Lazzeretti, J. Chem. Phys. **126**, 154111 (2007).

[67] T. Helgaker and P. Jørgensen, J. Chem. Phys. **95**, 2595 (1991).

[68] S. K. Wolff and T. Ziegler, J. Chem. Phys. **109**, 895 (1998).

[69] M. Krykunov, T. Ziegler, and E. van Lenthe, J. Phys. Chem. A **113**, 11495 (2009).

[70] E. van Lenthe and E. J. Baerends, J. Comput. Chem. **24**, 1142 (2003).

[71] R. Ditchfield, Mol. Phys. **27**, 789 (1974).

[72] K. Wolinkski, J. F. Hinton, and P. Pullay, J. Am. Chem. Soc. **112**, 8251 (1990).

[73] G. Schreckenbach and T. Ziegler, J. Phys. Chem. **99**, 606 (1995).

[74] K. Kashiwabara, S. Konaka, and M. Kimura, Bull. Chem. Soc. Jpn. **46**, 410 (1973).

[75] P. A. Akishin, V. P. Spiridonov, and A. N. Khodchenkov, Zh. Fiz. Khim. **33**, 20 (1959).

[76] V. P. Spiridonov, A. G. Gershikov, and B. S. Butayev, J. Mol. Struct. **52**, 53 (1979).

[77] K. Kashiwabara, S. Konaka, T. Iijima, and M. Kimura, Bull. Chem. Soc. Jpn. **46**, 407 (1973).

[78] T. Kupka, Magn. Reson. Chem. **46**, 851 (2008).

[79] T. Kupka, Magn. Reson. Chem. **47**, 210 (2009).

[80] See supplementary material at http://dx.doi.org/10.1063/1.3608153 for additionally constructed ADF basis sets and calculated atomic charges and molecular quadrupole moments of linear $HgL_2$ (L = Cl, Br, I, $CH_3$) compounds.

[81] E. Malkin, I. Malkin, O. L. Malkina, V. G. Malkin, and M. Kaupp, Phys. Chem. Chem. Phys. **8**, 4079 (2006).

[82] E. Malkin, M. Repisky, S. Komorovsky, P. Mach, O. L. Malkina, and V. G. Malkin, J. Chem. Phys. **134**, 044111 (2011).

[83] U. Edlund, T. Lejon, P. Pyykkö, T. K. Venkatachalam, and E. Buncel, J. Am. Chem. Soc. **109**, 5982 (1987).

[84] C. J. Jameson and J. Mason, *Multinuclear NMR*, edited by J. Mason (Plenum, New York, 1987).

[85] M. Kaupp, *Theoretical and Computational Chemistry. Relativistic Electronic Structure Theory, Part 2: Applications*, edited by P. Schwerdtfeger, Vol. 14 (Elsevier B.V., Amsterdam, 2004).

[86] J. Autschbach, Theor. Chem. Acc. **112**, 52 (2004).

[87] M. Bühl, M. Kaupp, O. L. Malkina, and V. G. Malkin, J. Comput. Chem. **20**, 91 (1999).

[88] L. K. Sanders and E. Oldfield, J. Phys. Chem. A **105**, 8098 (2001).

[89] A. A. Auer, J. Gauss, and J. F. Stanton, J. Chem. Phys. **118**, 10407 (2003).

[90] J. A. Tosell, Phys. Chem. Miner. **31**, 41 (2004).

[91] M. A. Sens, N. K. Wilson, P. D. Ellis, and J. D. Odom, J. Magn. Reson. **19**, 323 (1975).

[92] P. Peringer, Inorg. Chim. Acta **39**, 67 (1980).

[93] M. Delnomdedieu, D. Georgescauld, A. Boudou, and E. J. Dufourc, Bull. Magn. Reson. **11**, 420 (1989).

[94] I. Persson, M. Sandström, P. L. Goggin, and A. Mosset, J. Chem. Soc. Dalton Trans. 1597 (1985).

[95] I. Persson, M. Sandström, and P. L. Goggin, Inorg. Chim. Acta **129**, 183 (1987).

[96] M. Sandström, Acta Chem. Scand., Ser. A **32**, 627 (1978).